# Quantitative Pulse-Phase-Thermography for Masonry and Concrete Structures

Ralf ARNDT, Christiane MAIERHOFER, Mathias RÖLLIG, Federal Institute for Materials Research and Testing (BAM), Berlin, Germany

**Abstract**. An advanced quantitative approach of pulse-phase-thermography for non-destructive testing in civil engineering is described in this contribution. The characteristic frequency of the maximum phase-contrast between defects and sound areas is used as a means for the characterization of its depth.
The new approach is tested in the laboratory on concrete structures with defects of polystyrene. The surfaces of the structures were heated with IR-radiators for varying time periods.
The presented investigations were funded by the Deutsche Forschungsgemeinschaft (DFG) and were carried out in co-operation with the Technical University of Berlin (TUB).

## 1 Introduction

### *1.1 Motivation*

As described earlier [1] the combination of impulse- (IT) and lock-in-thermography (LT), called pulse-phase-thermography (PPT), is an ideal approach to qualitative active thermography in non-destructive testing in civil engineering (NDT-CE). In earlier publications of the authors and others this was sufficiently documented [2], [3].
In this contribution the quantitative approach of PPT in NDT-CE, that was firstly introduced in [4] and that is based on the frequency $f_{ch}$ of the maximum phase-contrast between sound and defects areas, is proven for applications in NDT-CE, e. g. for the quantification of defects in concrete and masonry structures. An advanced approach of quantitative PPT in CE was required due to the inaccuracy of the results obtained by the analysis of the blind frequency $f_b$ and the apparent blind frequency $f_{b'}$, (see chapter 1.3 or [5], [6] for details).
The measurements procedures of IT and PPT are otherwise the same for laboratory as well as for on-site measurements and are described shortly in the next section.

### *1.2 Impulse-thermography*

In IT a high energetic heat impulse is applied to the specimen and the surface temperature is monitored and analysed with an IR sensor, or sensor arrays, along time (as shown in figure 1, left). Information about delaminations and near surface voids is accumulated through the temperature difference between disturbed and undisturbed areas. Time and amount of the maximum temperature contrast during the cooling down process is used for the detection and partly quantification of defects. In combination with numerical simulations in some cases a full quantitative proposition e.g. of the thickness of concrete

cover is possible [7]. Because of the possibility of high power density of the heat impulse IT is quite useful for NDT-CE, by applying an adequate degree of energy and time to the thermographic measurements.
Quantitative IT in CE is based on the analysis of time $t_{max}$ of the maximum temperature-contrast $\Delta T_{max}$ of a defect and a sound reference area (see figure 1, right). This approach is described in detail elsewhere [8] and is not part of this contribution.

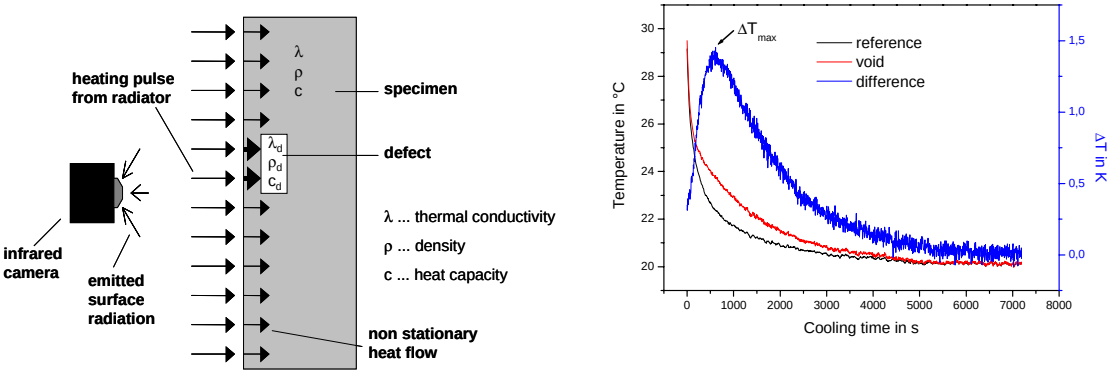


Figure 1: Principle of impulse-thermography (left side) and temperature difference curve ΔT (blue, right side) of transients of temperatures above a void $T_F(t)$ (red) and a reference point $T_R(t)$ (black).

## *1.3 Pulse-phase-thermography*

### *1.3.1 Qualitative pulse-phase-thermography*

In PPT the specimen is heated as in IT. The recorded temperature evolution is processed by performing Fast Fourier Transformation of the time signals of each recorded pixel at the surface. Thus, in addition to the information gained by IT in the time domain, the analysis is performed in the frequency domain. Amplitude and phase images are than used to extract information about the internal structure of an investigated specimen (see figure 2, left).

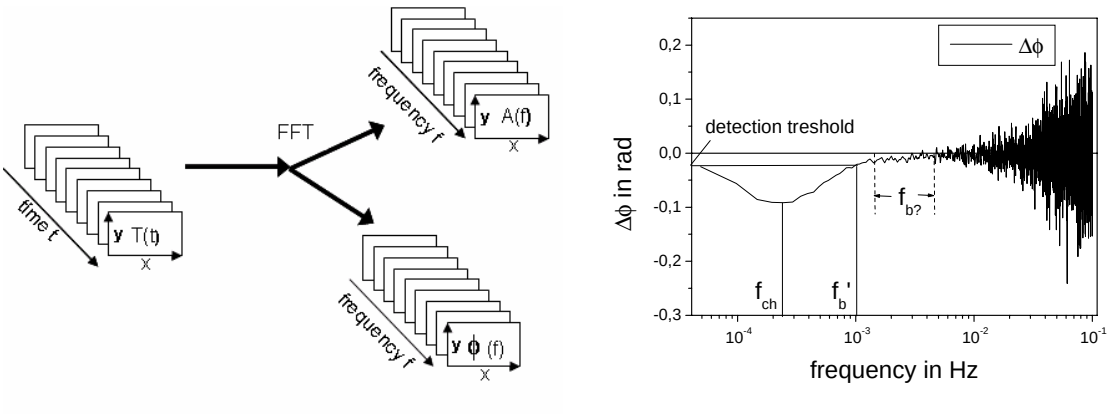


Figure 2: Principle of pulse-phase-thermography, Maldague [8] (left) and exemplary phase-contrast-curve $\Delta\varphi=\varphi_F-\varphi_R$ with $f_{ch}$, $f_b$ and $f_{b'}$ (right).

The main advantages of PPT are given by the following properties of the phase images [2]:

- Deeper probing as for amplitude images and thus enhanced detectability
- Less influenced by surface inhomogeneities
- Less sensitive to non-uniform heating
- Enhanced resolution of defect geometry
- Non-necessity to know a priori the position of non-defect area

in comparison to thermal images and amplitude images. This pre knowledge of non-defect areas is required for the computation of contrast images and difference curves in IT.
As a conclusion PPT is an ideal completion for a qualitative thermography in NDT-CE.

*1.3.2 Quantitative pulse-phase-thermography*

If a periodic thermal wave with a constant frequency f is assumed to propagate through a semi-infinite homogeneous material, the one-dimensional Fourier's Law can be solved analytically. From this solution, the diffusion length μ of the wave can be expressed as [9]:

$$\mu = \sqrt{\frac{\alpha}{\pi \cdot f}}. \tag{1}$$

Here, α is the thermal diffusivity α in [$m^2$/s].
Based on this equation, a relationship between the blind frequency $f_b$ (see figure 2, right side), at which a defect in a depth z in [m] becomes undetectable, can be related to the depth of the defect by [6]:

$$z = C_1 \cdot \sqrt{\frac{\alpha}{\pi \cdot f_b}}, \tag{2}$$

with the thermal diffusivity and the correlation constant $C_1$, which has shown to be equal to 1 for amplitude data and between 1.5 and 2 for phase data in [6]. Equation (2) clearly shows that defects can be detected from low frequencies up to the blind frequency, which depends on their depths. Consequently, shallow defects have a higher blind frequency than deeper defects and can be observed over a larger frequency range.
The accuracy for the determination of the blind frequency $f_b$ from the difference curve of the phases (as shown in figure 2, right) depends on geometry and thermal properties of the defects, but also on the data-recording in time domain. For achieving a high density of data points in frequency domain, the time window of the recorded temperature decay must be relatively large. Due to the already enhanced duration of measurement time at structures in civil engineering having low thermal conductivity, not in all cases the required long times for data acquisition can be realised. Therefore, before Fourier Transformation, the time data are enhanced by zero padding.
For badly sampled data it is very difficult to determine $f_b$. Here Ibarra-Castanedo [6] suggests an alternative approach to estimate a defects depth. It makes use of the *apparent blind frequency $f_b$'* (see figure 2, right side), which is based on establishing a minimum threshold value of the phase.
For a thermal wave, the phase ϕ is a function of depth and is given by the ratio of the depth and the diffusion length:

$$\phi = \frac{z}{\mu}. \tag{3}$$

Therefore, by applying a threshold value $\phi_{min}$ and a related apparent blind frequency $f_b$', equation (2) becomes [6]:

$$z = C_1' \cdot \phi_{min} \cdot \sqrt{\frac{\alpha}{\pi \cdot f_b'}} = C_1' \cdot \phi_{min} \cdot \mu'. \tag{4}$$

*$C_1$'* is the regression coefficient and μ'= $\sqrt{\frac{\alpha}{\pi \cdot f_b'}}$ the apparent diffusion length.

This approach works well for application to thin plates of metal or Plexiglas, but often fails in CE. Therefore, another alternative approach, based on the frequency of the maximum phase-contrast $f_{ch}$ (see figure 2, right side), was proposed in [4]:

$$z = f\left(\sqrt{\frac{\alpha}{f_{ch}}}\right) = k_c \cdot \sqrt{\frac{\alpha}{f_{ch}}} \tag{5}$$

with the correction factor $k_c$ analogue to $C_1$ in (1), that has to be quantified for varying boundary conditions.

## 2 Experimentals

### *2.1 Experimental set-up*

The experimental set-up for the performed IT-measurements is shown in figure 3, left.
It consists of a thermal heating unit (three IR-radiators with 2400 W power each), a commercial infrared camera (Inframetrics SC1000, 256x256 pixels in a wavelength range of 3-5 µm) and a computer system, which enables digital data recording in real time. The heating time was varied between 5, 10, 15 and 30 min and the observation time was 120 min with a computed frame rate of 0.2 Hz.
The resulting parameters for PPT/FFT are: maximum frequency $f_{max}$ =0.1 Hz, the number of frequency-steps $N_f = 2^{11}$ =2048 and the frequency-resolution $\Delta f = f_{max}/ N_f$=4.88179x$10^{-5}$ Hz (with zero-padding).

Figure 3: Experimental set-up for laboratory investigations at BAM with investigated specimen A.

### *2.3 Concrete test specimens*

#### *2.3.1 Investigated specimens*

For approving equation 5, investigations at two different concrete test specimens with defined defects were constructed. Specimen A has a size of 1.50 x 1.50 x 0.50 m³ and includes eight voids simulated by polystyrene cuboids with sizes of 20x20x10 $cm^3$ and 10x10x10 $cm^3$ (figure 4, left side). Specimen B has a size of 1.00 x 1.00 x 0.30 m³ with two polystyrene and two gas concrete (*Polysterol* and *Porenbeton,* German) cuboids with a size of 10x10x5 $cm^3$ and a concrete cover of 6 cm and 10 cm (figure 4, right side).
The thermal diffusivity of the concrete was estimated to be $\alpha$= 8.75 x $10^{-7}$ $m^2/s$.
Since the cuboids at specimen A shifted there positions during the concreting, radar-measurements were carried out. The calculated depths of the voids are shown in the last column of table 2. Since voids 3 and 4 shifted partly to the surface and are not parallel to the surface, they are not considered in the following investigations. In test specimen B, only the polystyrene cuboids are considered.

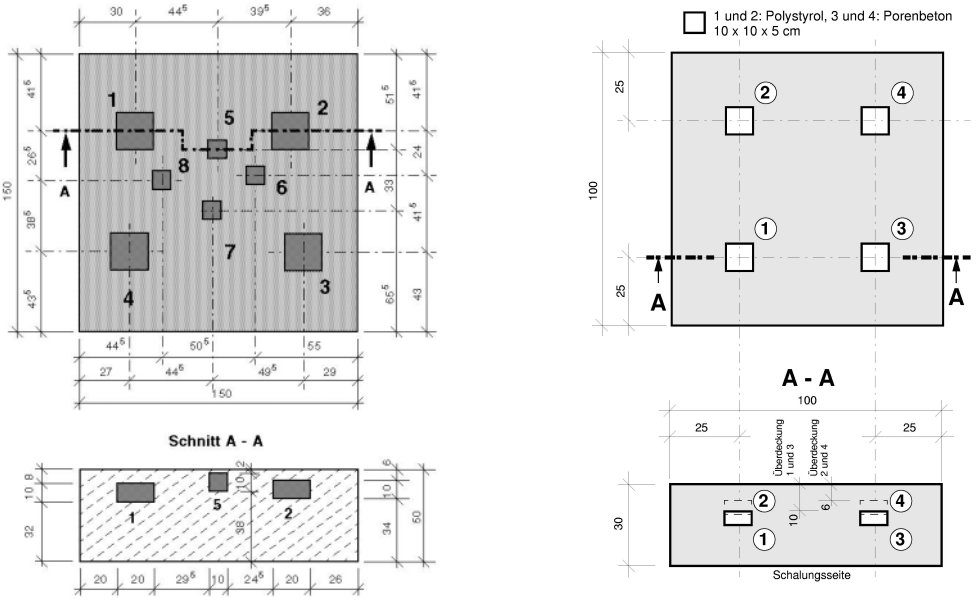


Figure 4: Concrete test specimen A (left) and B (right).

### *2.3.2 Experimental results*

Selected phase images of specimen A and B calculated from time series recorded after a heating time of 30 min are shown in figure 5, respectively. They are scaled to the maximum phase-contrast of void 1 (figure 5, left image, big void upper left) of specimen A and on void 2 (figure 5, right image, upper left) of specimen B.

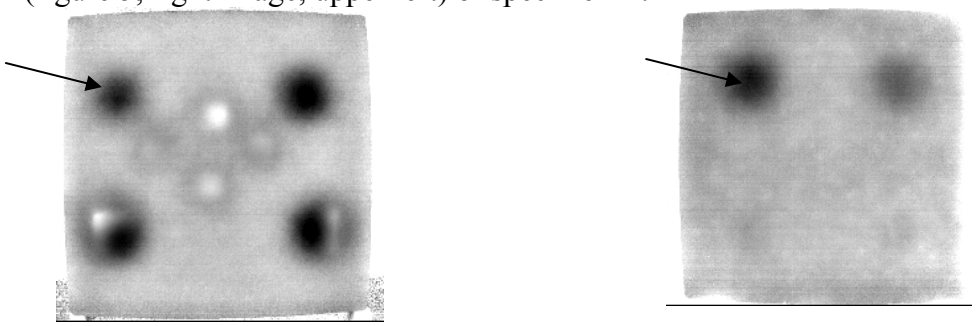

Figure 5: Phase images at $f_{ch}$ = 1.46 x $10^{-4}$ Hz of concrete test specimen A (left) and $f_{ch}$ = 2.44 x $10^{-4}$ Hz of concrete test specimen B for heating times of 30 min (right).

Figure 6 shows the phase-difference-curves (phase-difference as a function of frequency) for specimens A and B with heating times of 30, 15, 10 and 5 minutes.
It is evident that in these curves, $f_b$ or $f_b$' can only be determined with high inaccuracy, while the determination of $f_{ch}$ is much easier. One reason is the bad resolution at small frequencies.
As expected, the phase-difference-curves clearly show that $f_{ch}$ (frequency at the extremer – here minimum - of $\Delta\phi_{max}$) decreases with increasing depth (see for example AF2 and AF5), while the influence of the size of the voids (see for example AF1 and BF1) can be neglected (for the influence of the heating time on $f_{ch}$ see below).
The main influence on the absolute value of $\Delta\phi_{max}$ seems to lie in the size of the voids (again see AF1 and BF1) and the duration of the heating time in relationship to concrete cover, as can be observed e.g. for the shortest heating time of 5 min, where the phase contrast of the deeper voids is very low. Here, the heating duration was not long enough, thus at depths of 7 to 10 cm, the thermal front has not completely reached these voids.

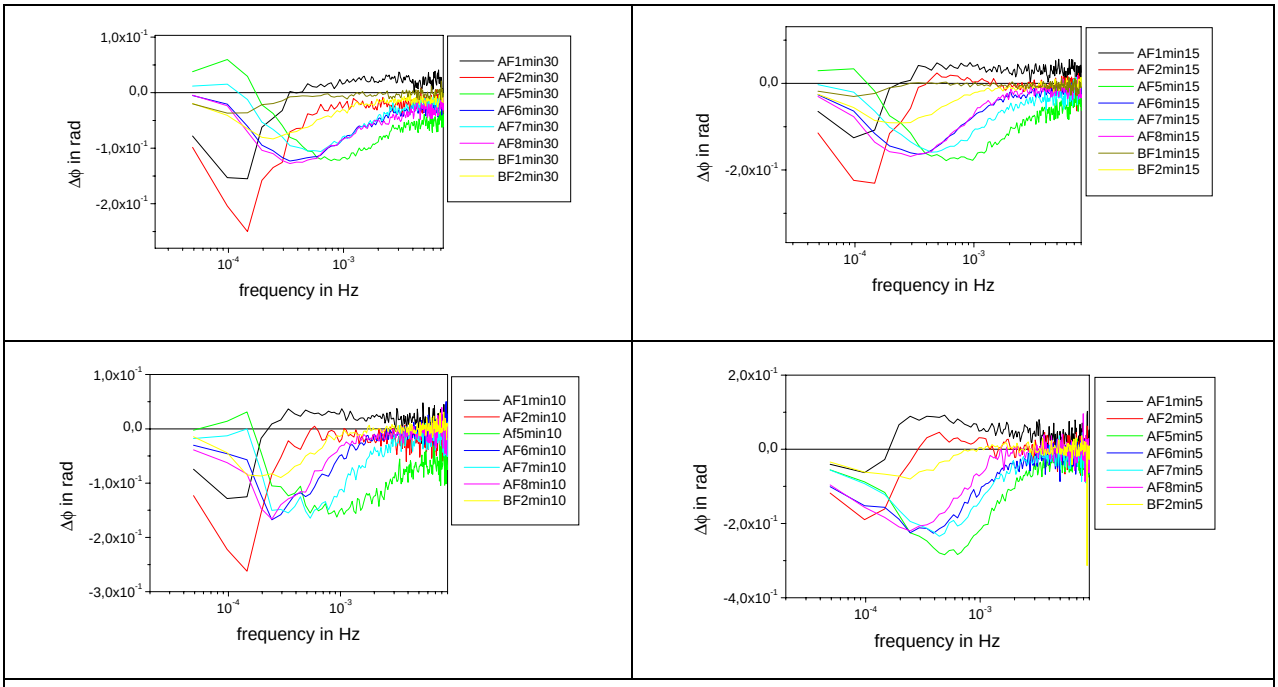


Figure 6: Phase-contrast-curves for the polystyrene voids of specimens A and B for 30 (left up), 15 (right up), 10 (left down) and 5 min (right down) of heating with an IR-radiator.

In figures 7 and 8, the real depths z (respective the concrete cover measured with radar) of the different voids are depicted over the factor $100 * \sqrt{\frac{\alpha}{f_{ch}}}$, which was determined from the phase difference curves in figure 6, for each heating time. These values are also summarised in table 2. Additionally, a linear fit was performed and the results of this correlation analysis are shown on top of the diagrams and are summarised in table 1.

**Table 1:** Correction factor $k_c$ for heating times of 30, 15, 10 and 5 min

| **Heating time** | **30 min** | **15 min** | **10 min** | **5 min** |
|---|---|---|---|---|
| **$k_c$** | 1.21878 | 1.20942 | 1.01737 | 0.95827 |

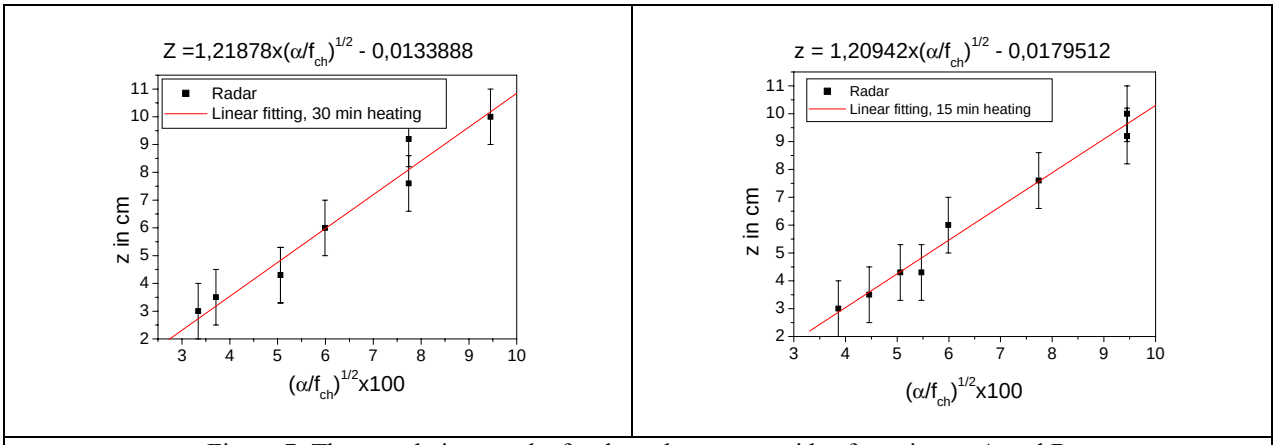


Figure 7: The correlation-results for the polystyrene voids of specimens A and B for 30 (left) and 15 min (right) of heating with an IR-radiator.

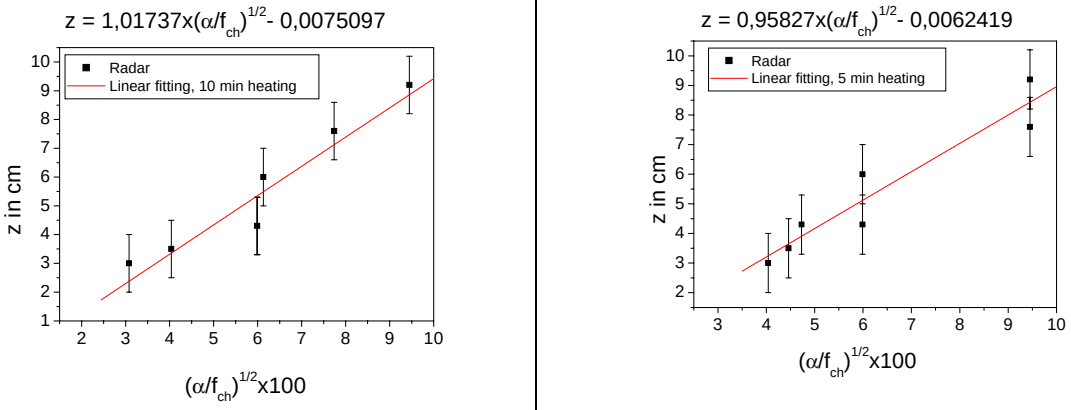


Figure 8: The correlation-results for the polystyrene voids of specimens A and B for 10 (left) and 5 min (right) of heating with an IR-radiator.

The presented results correspond greatly with the expectations and the influence of the heating time becomes obvious, although for the 10 minutes of heating the 4.3 cm deep defects fall out of the scale. With increasing heating time $k_c$ and the interception z, increases. As stated before a heating time of less than 10 minutes cannot be recommended for measurements of voids deeper than 6 cm and even for longer heating times the accurate estimation of concrete cover over 8 cm becomes difficult, without prolonging the observation time or increasing the frame rate to enhance the frequency-resolution.

Table 2 gives an overview of the used and calculated parameters following equation (3) for heating times of 5, 10, 15 and 30 minutes.

**Table 2:** Overview of the parameters for quantitative PPT for heating times of 30, 15, 10 and 5 min and with estimated α= 8.75 x 10-7 $m^2/s$ for concrete, the values in () were gained by using fit-functions.

| **Specimen/void** | **$f_{ch}$ in Hz x 10-4** | | | | **$\sqrt{\frac{\alpha_c}{f_{ch}}} \times 100$ in cm** | | | | **Concrete cover $c_{radar}$ or $_{nom}c$ in cm** |
|---|---|---|---|---|---|---|---|---|---|
| | **30 min** | **15 min** | **10 min** | **5 min** | **30 min** | **15 min** | **10 min** | **5 min** | |
| A/F1 | 1.46 | 0.98 | 0.98 | 0.98 | 7.74 | 9.45 | 9.45 | 9.45 | 9.2 ± 1.0 radar |
| A/F2 | 1.46 | 1.46 | 1.46 | 0.98 | 7.74 | 7.74 | 7.74 | 9.45 | 7.6 ± 1.0 radar |
| A/F5 | 7.81 | 5.86 | 9.28 | (5.36) | 3.34 | 3.86 | 3.08 | (4.04) | 3.0 ± 1.0 radar |
| A/F6 | 3.42 | 3.42 | 2.44 | 3.91 | 5.06 | 5.06 | 5.99 | 4.73 | 4.3 ± 1.0 radar |
| A/F7 | 6.35 | 4.39 | 5.37 | 4.39 | 3.71 | 4.46 | 4.04 | 4.46 | 3.5 ± 1.0 radar |
| A/F8 | 3.42 | 2,93 | 2.44 | 2.44 | 5.06 | 5.47 | 5.99 | 5.99 | 4.3 ± 1.0 radar |
| B/F1 | 0.98 | 0.98 | No value | No value | 9.45 | 9.45 | No value | No value | 10.0 |
| B/F2 | 2.44 | 2.44 | (2.31) | 2.44 | 5.99 | 5.99 | (6.15) | 5.99 | 6.0 |

## 3 Conclusions and outlook

PPT is a suitable enhancement for qualitative and for quantitative IT-measurements in CE. The new inverse approach for quantitative PPT via characteristic frequency is very useful for the estimation of concrete cover of 3 to 10 cm for at least 10 min of heating and to 5 cm with 5 min of heating with an IR-radiator and 2 hours of observation. It can easily be programmed into post processing algorithms for thermography measurements.
The methodology based on the maximum phase-contrast has one main advantage: $f_{ch}$ is unproblematic to locate as the SNR for $f_{ch}$ is higher then that for $f_b$ or $f_{b'}$ in all of the so far regarded cases of PPT in CE.
The only known disadvantage is, that the frequency-resolution for deep-lying defects becomes more inaccurate and requires longer observation times and/or bigger frame-rates, to enhance the frequency-resolution, at the cost of computing power and/or time resolution. Another option to optimize frequency-resolution is versa zero-padding, but that again needs computing power, which is often not available, especially for the usually big thermography data-sets. By optimising the measurement parameters, as frame-rate and observation time, corresponding to the depth to be quantified, this should be possible, as documented by [6]. Taking all this into account the results are very promising.
For a decided specification of heating times and conditions further-going investigations are momentarily carried out, that will be published elsewhere.

## Acknowledgements

The presented research was funded by the German Research Foundation (Deutsche Forschungsgemeinschaft, DFG).

## References

[1] Arndt, R., Maierhofer, Ch., Röllig, M., Weritz, F., Wiggenhauser, H.: Structural investigation of concrete and masonry structures behind plaster by means of pulse phase thermography, in: Proceedings of the 7th International Conference on Quantitative Infrared Thermography (QIRT), July 5 - 8, 2004, von Karman Institute, Rhode-St-Genese, Belgium.
[2] Maierhofer, Ch., Arndt, R., Röllig, M., Rieck, C., Walther, A., Scheel, H,. Hillemeier, B.: Application of impulse-thermography for non-destructive assessment of concrete structures, in CCC special Issue NDT 2006, in print.
[3] Weritz, F., Wedler, G., Brink, A., Röllig, M., Maierhofer, Ch. and Wiggenhauser, H.: Investigation of concrete structures with Pulse Phase Thermography, in: DGZfP (Ed.); International Symposium Non-Destructive Testing in Civil Engineering (NDT-CE) in Berlin, Germany, September 16-19, 2003, Proceedings on BB 85-CD, V80, 2003, Berlin.
[4] Arndt, R., Helmerich, H., Maierhofer, Ch., Röllig: Quantitative Pulse-Phase-Thermography for Composites and Concrete Structures, in: Proceedings of the Structural Faults and Repair - 2006, June 13 - 15, 2006, Edinburgh, Scotland, in print.
[5] Ibarra-Castanedo, C., Maldague, X.: Pulsed phase thermography reviewed. Quantitative Infrared Thermography Journal 2005; 1(1): 47-70.
[6] Ibarra-Castanedo, C.: Quantitative subsurface defect evaluation by pulsed phase thermography: depth retrieval with the phase, Phd-thesis, Université Laval, Canada, 2005, source: http://www.theses.ulaval.ca/2005/23016/23016.html.
[7] Maierhofer, C., Wiggenhauser, H., Brink, A., Röllig, M.: Quantitative numerical analysis of transient IR experiments on buildings, Infrared Physics and Technology 2004; 46: 173-180.
[8] Maldague, X.: Theory and practice of Infrared Technology for non-destructive testing, John Wiley and Sons, Inc., 2001.
[9] Wu, D., Wu, C. Y. and Busse, G.: Investigation of resolution in lock-in thermography: theory and experiment, in: Proceedings of QIRT 1996, Pisa: Edizioni ETS, 1997, pp. 269-274.